EnvironmentAsia
The international journal by the Thai Society of Higher Education Institutes on Environment

EnvironmentAsia 12 (Special issue) (2019) 36-47
DOI 10.14456/ea.2019.61
ISSN 1906-1714; ONLINE ISSN: 2586-8861

Assessment of the Lower Ping River's Riverbank Erosion and Accretion, Northern Thailand Using Geospatial Technique; Implication for River Flow and Sediment Load Management

Nikhom Chaiwongsaen*, Montri Choowong

Morphology of Earth Surface and Advanced Geohazards in Southeast Asia Research Unit (MESA RU), Department of Geology, Chulalongkorn University, Phayathai Road, Pathumwan, Bangkok, 10330, Thailand

*Corresponding author: Nchaiwon@hotmail.com

Abstract

The Lower Ping River downstream from the Bhumibol Dam has suffered from the excessive sedimentation. Rapid growth sandbars occur along the 129 km of the downstream reach within the succession of weirs. Severe riverbank collapses can also be detected locally. The objective of this research is to assess riverbank accretion/erosion using remote sensing and GIS techniques. Comparison of the 2007 and 2017 satellite images shows that total emerged island bar area increases up to 5,702,557 m^2. The total riverbank erosion area is 1,150,943 m^2 whereas the total of accretion area is over 10,561,530 m^2. Digital Shoreline Analysis System (DSAS) software was used to determine the riverbank erosion/accretion rates. The DSAS output shows the average rate of erosion and accretion at 1.24 and 4.89 m/year. Rapid growth of sandbars is responsible for the shallowing and narrowing of river embankment leading to rapid overflow during flooding. The result from this study enables all authorities and stakeholders to recognize the specific locations, which have severely been affected by riverbank accretion and erosion.

Keywords: Lower Ping River, Sandbar, Riverbank erosion/accretion, Succession of weir

1. Introduction

The irrigation system for the Ping River has been established since the early 50's. All development projects mainly involve flood mitigation, supplying water to farmlands, and hydroelectric power generation. The Bhumibol Dam completed since 1964 and the Lower Mae Ping Dam constructed in 1991 to be operated as an additional reversible hydropower plant system 5 km downstream of the Bhumibol Dam. In addition, a succession of 7 weirs has been installed within the past decade along the Ping River in Changwat Kamphaeng Phet and Nakhon Sawan. These irrigation projects have provided numerous socioeconomic benefits not only for agriculture in the irrigation areas, but also played the important role in flood control. When Bhumibol Dam was completed, it separates the Ping River into the Upper and Lower Ping Rivers. Nowadays, adverse effects on hydraulic and sediment regimes along the river due to irrigation projects have been recognized and documented (Baker *et al.*, 2010; Francis *et al.*, 2005; Magilligan and Nislow, 2005; Magilligan *et al.*, 2016; Renshaw *et al.*, 2014; Shields *et al.*, 2000; Yang *et al.*, 2003; Yang *et al.*, 2005). The Lower Ping River downstream from the Bhumibol Dam has also influenced by these adverse effects of the irrigation projects, as the flow of the Lower Ping River is highly altered by the presence of irrigation system and as one third of the catchment comprises of highly weathered and erodibility granite supplying enormous sedimentary budget into the river course (Chaiwongsaen *et al*., 2019). The sand-clogged river has worsened and seems to be accelerated in the past few decades, especially within the succession of weir. The aim of this study is to assess and quantify the changes of the Lower Ping River dynamics within the succession of weir in term of changing emerging sandbar surface, annual rate and areal changes of accretion/erosion of riverbanks during the past decade (Figure 1). The high construction rate of sandbars within the succession of weir is responsible for the shallowing and narrowing of river embankment, which is the one of the major causes for rapid overflow during flooding (Figure 2). The affected areas from riverbank accretion and erosion as well as huge river channel shifting from rapid growth of sandbar will be determined. This study result will shed light on how to sustainably manage the irrigation system especially construction of weir, riverbank collapse prevention, and management of intense in-channel sand mining along the river.

2. Materials and Methods

The assessment of the Lower Ping River's morphological changes within the succession of 7 weirs in term of riverbank accretion/erosion and emerging sandbar area were analyzed using geospatial technique. The Google Earth (GE) images during dry season dated of the 4/3/2007 and 4/27/2017 were used in this study. The reason that we selected the images from dry season for analysis is that they can demonstrate the changes of sandbars better than during wet season which may recorded during flood events. Moreover, The Lower Ping River has been regulated by both Bhumibol Dam and the Lower Mae Ping Dam. Monthly river flow during the period 1955-2018 at Station P.2A in Changwat Tak (Figure 2) were obtained (RID, 2018). It demonstrates that the Bhumibol and Lower Mae Ping Dams have completely controlled the discharge of the Lower Ping River. This makes the discharges are quite constant throughout the year. Decadal of riverbank line variation and emerging sandbars between 2007 and 2017 were extracted from these GE images. The advantage of using GE is that it provides the satellite imagery with high spatial resolution at different time periods which is very useful for study the dynamics of the Lower Ping River. The extraction of the GE images was operated by the Elshayal Smart software. The Elshayal Smart software can download the Google earth images along with the coordinate which can be imported directly by ArcMap without the need for georeferencing. A total of 60 images from 2007 and 2017 covering the entire study area were downloaded. With spatial resolution less than 1m, the riverbank lines and sandbar boundaries can be digitized in ArcMap. The change in emerging sandbar surface areas was performed by clipping operation between the digitized sandbar polygons from 2007 and 2017.

The accretion/erosion areas along the riverbanks also have been defined and calculated using basic clipping operation in ArcMap. Furthermore, the assessment of riverbank accretion/ erosion was analyzed using the Digital Shoreline Analysis System (DSAS) (Thieler *et al*., 2009). DSAS is free software used to calculate shoreline change statistics through vector data. It can be downloaded and used as an extension in ArcMap. This software is designed for coastal environments assessment, but it also can be adapted to use with other environments that show boundaries (Oyedotun, 2014) such as riverbank lines in this study. The riverbank lines generated from the GE were analyzed using DSAS software for measurement of accretion/erosion rate along the river segments (Misra and Balaji, 2015; Mujabar and Chandrasekar, 2011). DSAS can calculate numerous statistical analyses based on the changes in accretion/erosion rates of riverbank. However, only two main statistical analyses including Net Shoreline Movement (NSM) and End Point Rate (EPR) were used in this study. DSAS uses a measurement baseline

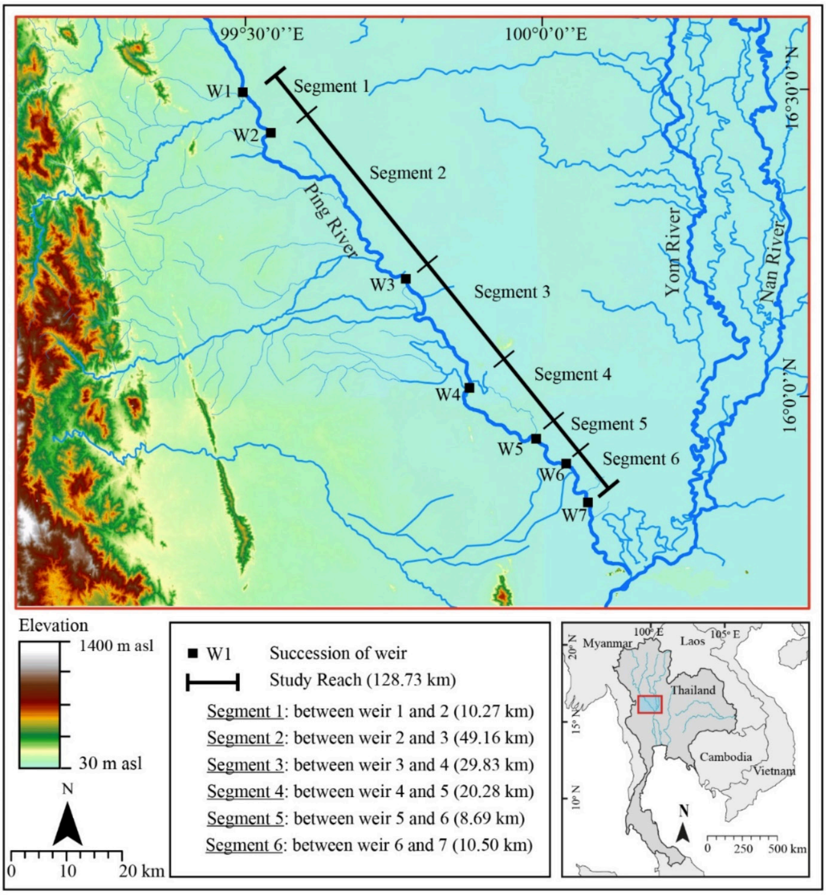

Figure 1. Map of the study area showing the succession of weir along the Lower Ping River and 6 segments of this study

method to calculate rate-of-change statistics for a time series of riverbank lines. The baselines were constructed by create buffer of the 2017 riverbank lines. They were established 200 m on land adjacent to the riverbank lines of both river sides. DSAS computes the riverbank line change by generating transects perpendicular to the baselines and intersect all riverbank lines. We used the transect spacing of 50 m along the riverbank and the length of transect line at 700m. Transects establish measurement points between both riverbank lines. The option of "Smoothed Baseline" was used in this study as it is suitable for orienting transects along curved sections of baseline along the riverbank line. The distances between the 2007 and 2017 riverbank lines were calculated as NSM (the net change distance) and the EPR calculated by dividing the NSM by the number of years between the both riverbank lines, which is 10 years in our study. The negative NSM or EPR values indicate erosion while positive values indicate accretion.

3. Results and Discussion

3.1 Change in emerging sandbar area

The succession of weir of the Lower Ping River starts from the Weir #1 located at latitude 16°30′1″N and longitude 99°29′42″E and ends at the Weir #7 (latitude 15°49′47″N and longitude 100°4′29″E) 15 km above the Ping-Nan confluence (Pak Nam Poh) in Changwat Nakhon Sawan. These weirs have been built within this reach in order to raise the river water level and diverse the water for irrigation purpose. The direct adverse effect of weir is increasing sediment deposition and formation of sandbar behind them (Lane and Richards, 1997). Table 1 shows that the total area of the island bars had dramatically increased 5,702,557 m^2 (25.61%) between 2007-2017. The maximum increasing percentage of 45% was in the Segment 1 and 6. In all segment, the small island bars tend to grow or merge into larger island bars within the river embayment, or as point or lateral bars attached to riverbanks through time (Figure 4 and 5).

3.2 Change in accretion/erosion area

The calculated values of the accretion/erosion area of the Lower Ping River's riverbank are shown in Table 2. The analysis of areal change per 1 km of riverbank is demonstrated in Figure 6. All locations of riverbank accretion/erosion are illustrated in Figure 7. The values in Figure 6 were calculated as "accretion/erosion areal change per 1 km" along both riverbank of the river. This has been done by divided the accretion/erosion areal change value of each

Table 1. Calculated emerge island bar surface areas from all segment from 2007 and 2017

Segment	Length (km)	Emerging sandbar area (m²)		Increasing area (m²)	Increasing area (%)
		2007	2017		
1	10.27	881,800	1,283,205	401,405	45.46
2	49.16	9,694,005	12,220,500	2,526,495	26.06
3	29.83	5,414,911	6,788,780	1,373,869	25.37
4	20.28	3,440,846	3,960,288	519,442	15.08
5	8.69	1,268,297	1,441,836	173,539	13.72
6	10.50	1,568,425	2,276,232	707,807	45.15
Total	128.73	22,270,291	27,972,858	5,702,557	25.61

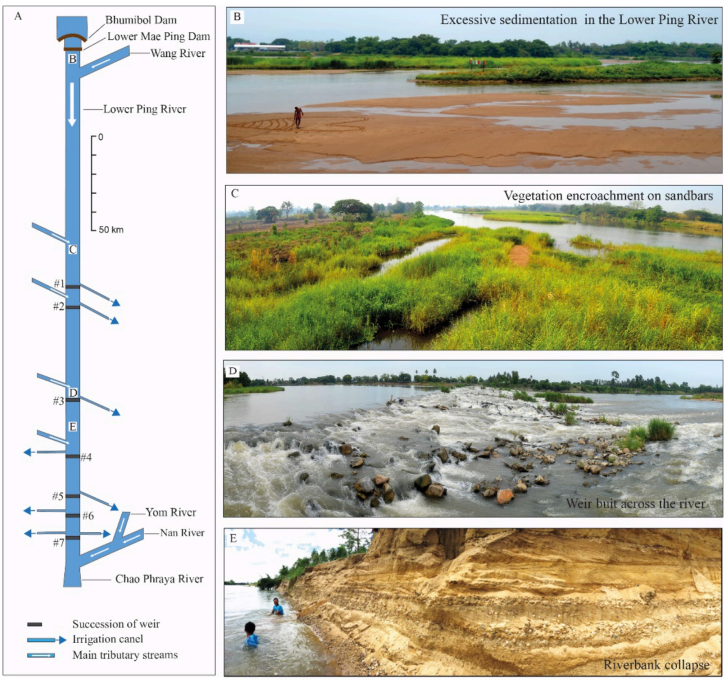

Figure 2. A) the illustration drawing of the Lower Ping River; B) excessive sedimentation along the river, C) vegetation encroachment on sandbars, D) Weir # 3 of the succession of weir, E) severe riverbank erosion of the Lower Ping River

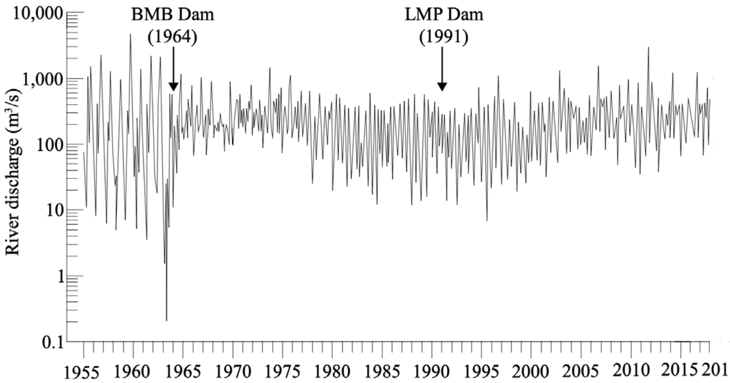

Figure 3. The history of the Ping River's discharge during 1955 to 2018

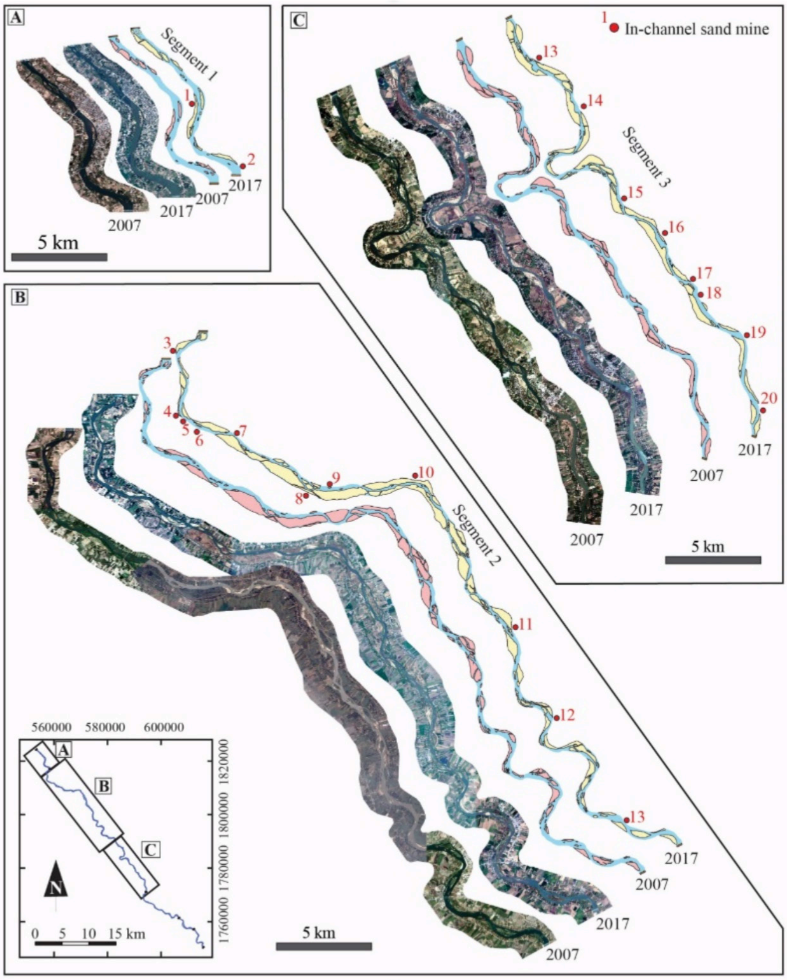

Figure 4. Maps showing sandbars deposited during 2007 and 2017 with the locations of existing in-channel sand mine; A) along segment 1, B) along segment 2, and C) along segment 3

Table 2. The calculated accretion/erosion areas of the riverbank

Segment	Right riverbank		Left riverbank	
	Accretion (m^2)	Erosion (m^2)	Accretion (m^2)	Erosion (m^2)
1	325,054	8,035	85,551	71,718
2	1,463,541	500,977	1,772,124	533,688
3	2,017,010	190,419	1,409,340	161,659
4	907,786	171,453	867,045	73,723
5	118,841	254,660	243,460	31,168
6	430,676	25,399	921,102	51,932
Total	5,262,908	1,150,943	5,298,622	923,888

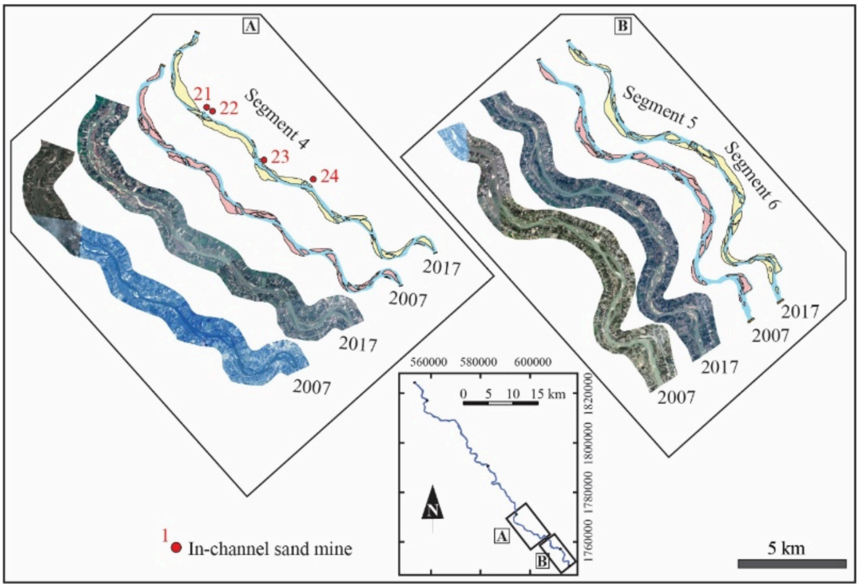

Figure 5. Maps showing sandbars deposited during 2007 and 2017 with the locations of existing in-channel sand mine; A) along segment 4, and B) along segments 5 and 6

segment with the segment length. The result shows that the maximum erosion areal change i.e. most severe riverbank collapse is 29,304 m^2/km on the right riverbank of segment 5. This is probably due to there is no main tributaries within this segment to supply more sediment budget into the river. The maximum accretion areal change i.e. most aggradation occurs on the left riverbank of the segment 6 with the value of 87,724 m^2/km. Since this is the last segment downstream of the river, it tends to have lower gradient than the upstream segment. Moreover, the 6 weirs installed upstream have reduced the flow velocity. Hence combination of low river gradient and low flow velocity will promote construction i.e. accretion of point and lateral bars within this segment. The total riverbank accretion area is 5,298,622 m^2 on the left riverbank and 5,262,908 m^2 on the right riverbank. The total riverbank erosion area is 1,150,943 m^2 on the right riverbank and 923,888 m^2 on the left riverbank. This result indicates that the Lower Ping River along the succession of weir had tremendous increased point/lateral bars with the total accretion area of 10,561,530 m^2 which is 5 times over the total erosion area of 2,074,831 m^2.

3.3 Riverbank accretion/erosion rate

DSAS is used in analyzing the rate of riverbank line changes between 2007 and 2017 GE images. Two statistical values from the analysis include NSM and EPR. The analysis has been operated separately for each segment and for the left and right side of the riverbank. The NSM values (distances between the 2007 and 2017 riverbank lines) were divided by 10 to calculate the accretion/erosion rate per year (EPR). The EPR values for all transect lines were imposed on the areas of accretion/erosion as shown in Figure 7. The EPR values indicate the instability of each study segment. The high EPR value implies that the riverbank line shifting is high either from accretion or erosion. The highest average accretion rate is 14.63 m/y on the right riverbank of segment 6, whereas highest average erosion rate is -6.04 m/y on the right riverbank of segment 5 (Table 3). The accretion/erosion rates of the right riverbank for the entire river reach (from Weir #1 to #7) are 5.21 and -1.66 m/y, whereas on the entire left riverbank are 4.52 and -0.77 m/y. The overall average of riverbank accretion/erosion rates (both right and left riverbank combined) are 4.89 and -1.24 m/y. This suggests that the right riverbank of the Lower Ping River had undergone greater shifting than the left side. It also indicates that the river reach had been under high aggradation stage during 2007-2017. This results in significant river shallowing and narrowing only within a decade timespan.

3.4 The possible factors responsible for the rapid accretion/erosion of riverbank

River morphological changes through riverbank and bed erosion and riverbank accretion, which are natural processes. Normally, river riverbank erosion and sandbar deposition take amount of timespan to shape the river morphology, however anthropogenic activities such as sand mining, riverbank revetment, and construction of irrigation structures can accelerate the changes (Fuller *et al.*, 2003; Li *et al.*, 2007; Rinaldi, 2003; Surian and Rinaldi, 2003). The combination of high sediment supply and low water discharge is believed to be the cause for excessive sediment deposit along the Lower Ping River within the succession of weir. As one-third of the Lower Ping Catchment comprises of highly weathered and high erodibility granite, enormous amount of sediment budget has been supplied to the Lower Ping River through the main tributary streams on the western side of the river (Chaiwongsaen *et al.*, 2019). If a weir has been installed downstream close to the confluence, it will accelerate more sandbar accretion than the one installed further from the confluence. This high sedimentation rate reflected in rapid growth of sandbar (Figure 8 and 9). The GE images has revealed that within only one decade (2007-2017) the Lower Ping River between the succession of weir has rapid growth sandbars throughout the river course. This acceleration of sandbars construction seems to coincide with

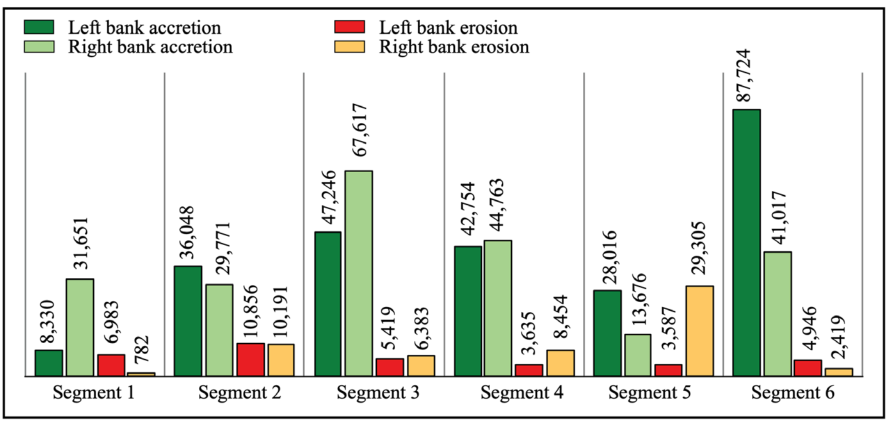

Figure 6. Graph of accretion/erosion area per km (m^2/km) for both sides of riverbank of each segment

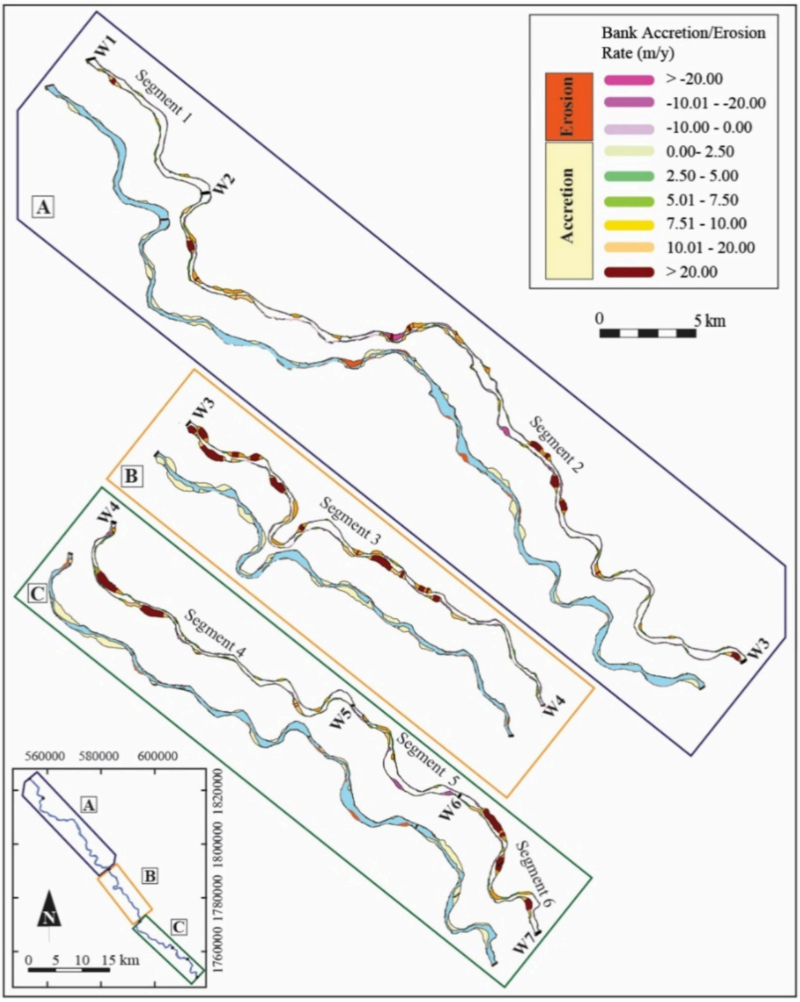

Figure 7. Map showing accretion area (yellow) and erosion area (orange) of the riverbank line and the End Point Rate (EPR) of these accretion/erosion areas in m/y

Table 3. The accretion/erosion rate of riverbank line (EPR values calculated from DSAS)

Segment	Right riverbank EPR rate (m/y)				Left riverbank EPR rate (m/y)			
	Accretion		Erosion		Accretion		Erosion	
	Max.	Average	Max.	Average	Max.	Average	Max.	Average
1	23.89	4.09	-3.23	-0.69	11.18	2.88	-2.80	-1.08
2	39.68	5.80	-25.53	-2.22	28.09	6.64	-30.88	-2.83
3	36.65	12.97	-8.00	-2.38	32.81	7.89	-7.66	-1.77
4	38.24	6.81	-12.53	-3.36	40.67	6.33	-8.09	-1.34
5	16.43	2.74	-17.68	-6.04	18.09	5.12	-4.21	-1.00
6	29.89	5.36	-5.98	-1.22	31.75	14.63	-7.96	-1.32
All	39.68	5.21	-25.53	-1.66	40.67	4.52	-30.88	-0.77

a time frame of the succession of weir which initiated during the past decade. A construction of weir makes grade of the stream suddenly raised, which changes the stream bed profile and sedimentation along the regulated river course (Leopold, 1992). When the weir completed, a reservoir is formed upstream and then gradually filled with sediment transported down by the stream. Trapped sediment load within the succession of weir accelerate sedimentation i.e. sandbar construction. Figure 1, and 2 demonstrates that the mountain rages on the west of the Lower Ping River have supplied sediment budget into the river through tributary streams. This increases sedimentation along this river reach many folds. Figure 8 shows that the accretion and erosion of riverbanks are related. At the point where rapid growth point bar occurs, the riverbank on the opposite side also has encountered the acceleration of riverbank collapsing. The rapid growth of sandbar abruptly changes the river flow direction and increases the flow velocity, which poses a threat to riverbank on the opposite side.

The shallowing and rapid accretion of riverbank sometimes also cause problems for fixed-based pump stations installed along the river reach by lower the water level below the propeller and sump levels of several pump stations. This makes them cannot be operated properly (Figure 8E). Another factor that can cause severe riverbank erosion is over exploitation of sand and gravel by in-channel sand mining. In-channel sand mining creates

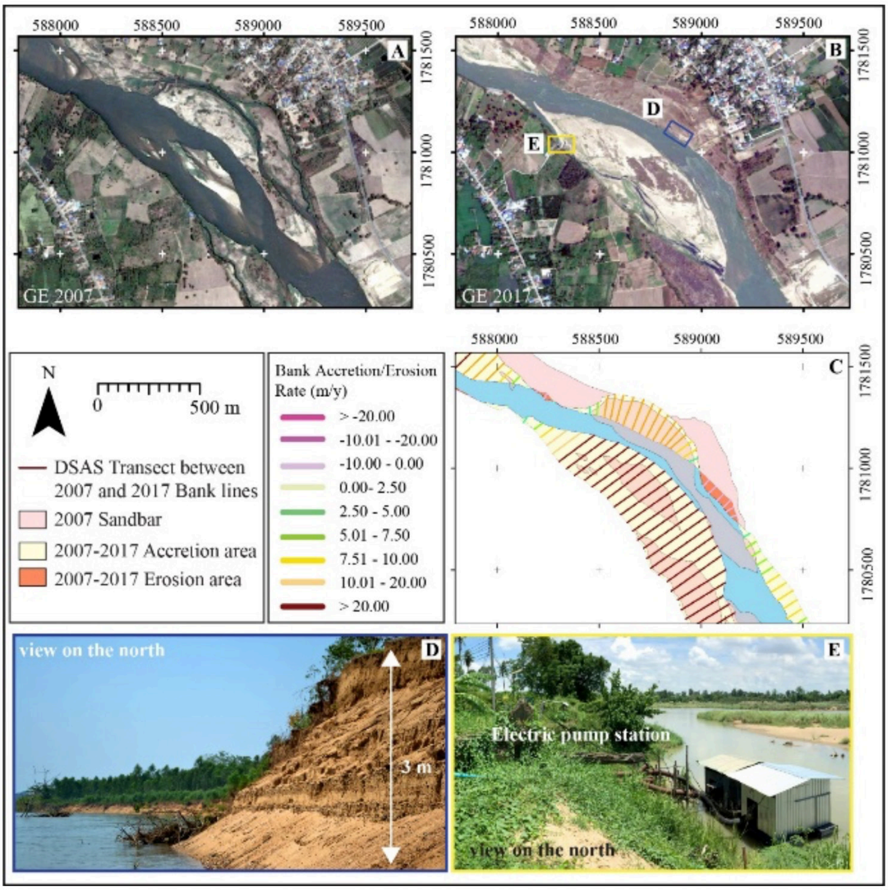

Figure 8. A) and B) the GE images showing example of a rapid growth sandbar, C) the illustration showing EPR rates of the river riverbank imposed on the accretion/erosion areas, D) the severe riverbank collapse, and E) The shallowing and rapid accretion of riverbank cause problems for pump stations

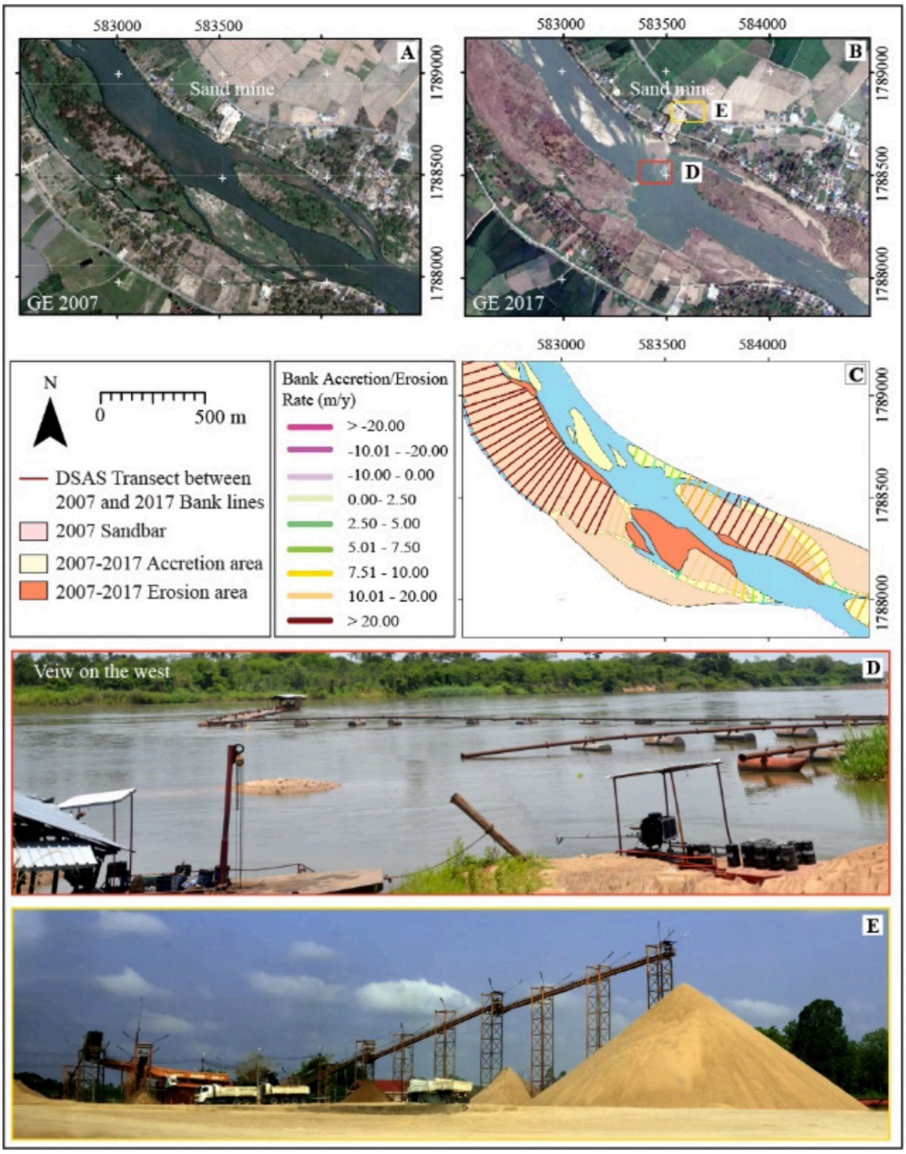

Figure 9. Map showing effect of in-channel mining on riverbank erosion; A) and B) comparison of riverbanks and sandbar from GE images in 2007 and 2017, C) the EPR rates of the river riverbank are imposed on the accretion/erosion areas, D) and E) the operation of in-channel sand mining

deep ponds on the river bed which resulting in obvious loss of sandbars around them (Fig. 8).

3.5 Implications

The implications from this study can distribute to both hydraulic and sediment regimes management. In Thailand, weirs are very useful and have been used as one of the fundamental irrigation structures to control rivers and streams for centuries. They have been mainly constructed for raising water level and diverting flows through irrigation canals for farmlands. This study suggests that within the high sedimentation river such as the Lower Ping River, construction of weir will have significant adverse effect which is trapping bedload sediment behind them causing river shallowing and narrowing. Hence weir construction requires studies of geologic conditions, location of weir correlation with tributaries, and sediment budget characteristics. Furthermore, building a succession of weir along high sedimentation river will generate more adverse impacts on the river.

The Lower Ping River course within the succession of weir has trapped enormous sand sediment. This results in intensive in-channel sand mining in this area. There are at least 24 sand mines distributed along the Lower Ping River (Figure 3 and 4). The intense in-channel sediment mining within the Lower Ping River has created conflict among stake holders. Even though, the Lower Ping River has high availability of sand and gravel due to excessive sedimentation. But over exploitation rate of in-channel sand mining causes severe riverbank erosion (Figure 9). The results of this study locate and determine the affected areas from riverbank accretion and erosion as well as huge river channel shifting from rapid growth of sandbar. This assists authority to locate the suitable in-channel mining sites by excluding these high erosion rate areas. In addition, the locations of high accretion/erosion riverbank rate determined from this study will be useful for the riverbank collapse prevention.

4. Conclusions

The Lower Ping River's morphology has changed dramatically and unusually over years. Erosion usually occurs on the outside bend of the river whereas sediment deposits on the inside bend. However, for the high aggradation stage river like this Lower Ping River the process of deposition will be accelerated which results in more island bars construction and rapid accretion of point bars. Analysis of Google Earth images of 2007 and 2017 clearly illustrates tremendous change of river morphology and emerging sandbars and displays accretion and erosion of the riverbanks. Combined remote sensing and GIS techniques in this study demonstrates an efficient mean of determining river dynamics. It shows that during this decadal timespan the Lower Ping River within the succession of weir had significantly increased emerging sandbars and riverbank accretion areas. However, at points where rapid growth point bars occur, the riverbank on the opposite side also has severe riverbank erosion. The rapid growth of sandbar changes river flow direction and increases flow velocity, which poses a threat to riverbank on the opposite side. Both increasing of sandbar area and accretion of riverbank lines indicate that the reach is very active and unstable. Trapping enormous amount of sand and gravel within the succession of weir together with high sediment supply from the mountain ranges on the west are responsible for the unusually high aggradation of the Lower Ping River. This study also provided statistics of accretion/erosion rates using geospatial technique of DSAS. The areas of high accretion/erosion rates were detected and located along the riverbanks. These insights will assist management of the water and sediment of the Lower Ping River, and to ensure that these resources will be utilized sustainably.

Acknowledgements

We are deeply grateful to the research grant provided by the 90th Anniversary of Chulalongkorn University. We also would like to acknowledge National Research Council of Thailand (NRCT) for funding this project via Agricultural Research Development Agency (Public Organization), (ARDA). Many thanks to people whom directly or indirectly involved by sharing ideas and providing technical support, throughout this project.

References

Baker, D.W., Bledsoe, B.P., Albano, C.M. and Poff, N.L. Downstream effects of diversion dams on sediment and hydraulic conditions of Rocky Mountain streams. River Res Appl. 2010: 27; 388-401.

Chaiwongsaen, N., Nimnate, P. and Choowong, M. Morphological Changes of Sand Bar from the Lower Ping and Chao Phraya Rivers, North and Central Thailand: Flood and Coastal Equilibrium Analyses. Open-Geosciences. 2019: 11; 152-171.

Francis, J., Magilligana, T. and Nislow, K.H. Changes in hydrologic regime by dams. Geomorphology. 2005: 71; 61-78.

Fuller, I.C., Large, A.R.G. and Milan, D.J. Quantifying channel development and sediment transfer following chute-off in a wandering gravel-bed river. Geomorphology. 2003: 54; 307–323.

Lane, S.N. and Richards, K.S. Linking river channel form and process: time, space and causality revisited. Earth Surf. Process. Landf. 1997: 22; 249–260.

Leopold, L.B. Base Level Rise: Gradient of Deposition. Israel Journal of Earth Sciences. 1992: 41; 57-64.

Li, L.Q., Lu, X.X. and Chen, Z. River channel change during the last 50 years in the middle Yangtze River: an example of the Jianli reach. Geomorphology. 2007: 85; 185–196.

Magilligan, F.J. and Nislow, K.H. Changes in hydraulic regime by dams. Geomorphology. 2005: 71; 61-78.

Magilligan, F.J., Nislow, K.H., Kynard, B.E. and Hackman, A.M. Immediate changes in stream channel geomorphology, aquatic habitat, and fish assemblages following dam removal in a small upland catchment. Geomorphology. 2016: 252; 158–170.

Misra, A. and Balaji, R. A study on the shoreline changes and Land-use / land-cover along the South Gujarat coastline. Procedia Eng. 2015: 116; 381-389.

Mujabar, S. and Chandrasekar, N. A shoreline change analysis along the coast between Kanyakumari and Tuticorin, India, Using Digital Shoreline Analysis System. Geo-spatial Inf Sci. 2011: 14(4); 282-283.

Oyedotun, T.D.T. Shoreline Geometry: DSAS as a Tool for Historical Trend Analysis. Geomorphol. Tech. (online Ed.). 2014: 2; 1-12.

Renshaw, C.E., Abengoza, K., Magilligan, F.J., Dade, W.B. and Landis, J.D. Impact of flow regulation on near-channel floodplain sedimentation. Geomorphology. 2014: 205; 120-127.

RID. 2018. Lower Northern Region Irrigation Hydrology Center, the Royal Irrigation Department: 2018 Monitoring Report. [Available from: https://www.hydro-2.com]

Rinaldi, M. Recent channel adjustments in alluvial rivers of Tuscany, Central Italy. Earth Surf Process Landf. 2003: 28; 587–608.

Shields, F.D.J., Simon, A. and Steffen, L.J. Reservoir effects on downstream river channel migration. Environmental Conservation. 2000: 27(1); 55-66.

Surian, N. and Rinaldi, M. Morphological response to river engineering and management in alluvial channels in Italy. Geomorphology. 2003: 50; 307–326.

Thieler, E.R., Himmelstoss, E.A. and Ergul, A. Digital Shoreline Analysis System (DSAS) version 4.0 — An ArcGIS extension for calculating shoreline change. U.S. Geological Survey Open-File Report. 2009: 2008-1278.

Yang, S.L., Belkin, I.M., Belkina, A.I., Zhao, Q.Y., Zhu, J. and Ding, X.D. Delta response to decline in sediment supply from the Yangtze River: Evidence of the recent four decades and expectations for the next half-century. Estuarine Coastal Shelf Sci. 2003: 57(589–599).

Yang, S.L., Zhang, J., Zhu, J., Smith, J.P., Dai, S.B., Gao, A. and Li, P. Impact of dams on Yangtze River sediment supply to the sea and delta intertidal wetland response. J. Geophys. Res. 2005: 110; F03006.